Study on guided-mode resonance characteristic of multilayer dielectric grating with broadband and wide using-angle*

Wang Jian-Peng(汪剑鹏)[a)b)†], Jin Yun-Xia(晋云霞)[a)], Ma Jian-Yong(麻健勇)[a)b)], Shao Jian-Da(邵建达)[a)], and Fan Zheng-Xiu(范正修)[a)]

[a)] *Key Laboratory of Material Science and Technology for High Power Lasers, Shanghai Institute of Optics and Fine Mechanics, Chinese Academy of Sciences, Shanghai* 201800, *China*
[b)] *Graduate School of Chinese Academy of Sciences, Beijing* 100039, *China*

(Received 20 October 2009; revised manuscript received 16 November 2009)

Guided-mode resonance in a diffraction band of multilayer dielectric gratings may lead to a catastrophic result in laser system, especially in the ultrashort pulse laser system, so the inhibition of guided-mode resonance is very important. In this paper the characteristics of guided-mode resonance in multilayer dielectric grating are studied with the aim of better understanding the physical process of guided-mode resonance and designing a broadband multilayer dielectric grating with no guided-mode resonance. By employing waveguide theory, all guided-wave modes appearing in multilayer dielectric grating are found, and the incident conditions, separately, corresponding to each guided-wave mode are also obtained. The electric field enhancement in multilayer dielectric grating is shown obviously. Furthermore, from the detailed analyses on the guided-mode resonance conditions, it is found that the reduction of the grating period would effectively avoid the appearing of guided-mode resonance. And the expressions for calculating maximum periods, which ensure that no guided-mode resonance occurs in the requiring broad angle or wavelength range, are first reported. The above results calculated by waveguide theory and Fourier mode method are compared with each other, and they are coincident completely. Moreover, the method that relies on waveguide theory is more helpful for understanding the guided-mode resonance excited process and analyzing how each parameter affects the characteristic of guided-mode resonance. Therefore, the effects of multilayer dielectric grating parameters, such as period, fill factor, thickness of grating layer, *et al.*, on the guided-mode resonance characteristic are discussed in detail based on waveguide theory, and some meaningful results are obtained.

Keywords: multilayer dielectric grating, guided-mode resonance, broad band
PACC: 4225, 4225G

1. Introduction

The advent of the chirped-pulse amplification (CPA) technique ensures the realization of the high-power laser output.[1] As a critical element in CPA system for stretching and recompressing the pulse, grating is required to have a nearly 100% diffraction efficiency in –1st reflected diffraction order and to be able to endure high laser flux. In 1995, Lawrence Livermore National Laboratory (LLNL) first reported on the multilayer dielectric grating (MDG) model, which includes a high-reflectance (HR) multilayer thin film and a surface-relief grating.[2] The diffraction efficiency of the MDG could be more than 99.9% theoretically, and it was achieved to be more than 98% experimentally.[3,4] The laser-induced damage threshold (LIDT) of MDG was obtained to be more than 5 J/cm^2.[5] With high-efficiency and high LIDT, MDGs have been widely used in high-power laser systems. In recent years, Flury *et al.*[6−9] have obtained high-efficiency, broad band pulse compression gratings (PCGs) that include all-dielectric and metal-dielectric grating models. Based on these work, PCG with a broad band can be employed in ultrashort pulse laser system.

But it is noticed that there may be a guide-mode resonance (GMR) phenomenon in MDGs.[10] GMR shows the rapid intensity variation of propagation wave which is diffracted by a grating. The GMR has been a hot topic and widely researched in recent years, and some researchers have designed the resonant grating filters with the GMR.[11−16] But the GMR brings some catastrophic results to the MDG in a CPA system. Because of existence of GMR, the spectral shape

*Project supported by the National Natural Science Foundation of China (Grant No. 10704079).
†Corresponding author. E-mail: janpo@siom.ac.cn
© 2010 Chinese Physical Society and IOP Publishing Ltd

of laser pulse can be destroyed as it passes through the CPA system, furthermore, the electric field in the MDG can be enhanced greatly, which results in a low LIDT of MDG.[17] Ma *et al.*[18] has discussed the relation between GMR and fabrication error by using the Fourier mode theory. However, only the numerical results were obtained, and the physical mechanism of those results is still unclear. Therefore, the understanding of the physical process of GMR and how each parameter does affect the GMR character becomes a significant subject for the design of broad band MDG with no GMR.

In the present paper, the GMR characteristic in MDG is studied based on the waveguide theory.[19] All guided-wave modes supported by MDG system are presented, and based on the GMR condition, the incidence conditions (both in angle and in wavelength), separately, corresponding to each guided-wave mode are obtained. By comparing the results calculated from the waveguide theory and the Fourier mode method (FMM),[20] the two results coincide with each other completely. Moreover, the waveguide theory is more helpful for understanding the physical process of GMR and for analysing how each parameter affects the characteristic of GMR. The relations between GMR characteristic and some main parameters of grating such as period, fill factor and thickness of grating layer, are discussed, and some meaningful results are obtained. The necessary excitation conditions for GMR in MDG structure are presented by analysing the GMR conditions, and it is found that reducing grating period can inhibit the GMR effectively. These results are greatly helpful for designing a broad-band high-efficiency MDG.

2. Waveguide theory

GMR shows the rapid variation of amplitude diffracted by the reflection or transmission of MDG, which is due to the resonance of externally diffracted waves with the waveguide modes inside MDG. So in this section, we present the waveguide theory for calculating the waveguide modes which can be supported by MDG system.

An MDG is composed of two subsystems: a surface-relief grating and a multilayer high-reflection (HR) stack. It is located between the cover layer, which always is air, and substrate as shown in Fig. 1. According to the effective medium theory (EMT), the sub-wave grating periodic structure can be replaced with an isotropic homogeneous medium. So the MDG system can be treated as an asymmetric planar waveguide model. The effective indices of TE- and TM-polarizations are given by the EMT as the following equations:[14]

$$\varepsilon_{\mathrm{eff,TE}} = f\varepsilon_{\mathrm{l}} + (1-f)\varepsilon_{\mathrm{g}}, \tag{1}$$

$$\varepsilon_{\mathrm{eff,TM}} = \frac{\varepsilon_{\mathrm{l}}\varepsilon_{\mathrm{g}}}{f\varepsilon_{\mathrm{l}} + (1-f)\varepsilon_{\mathrm{g}}}, \tag{2}$$

where f is the grating filling factor, and ε_{l} and ε_{g} are the relative permittivities of the grating line and groove materials, respectively, $\varepsilon_{\mathrm{l}} = n_{\mathrm{l}}^2$ and $\varepsilon_{\mathrm{g}} = n_{\mathrm{g}}^2$. Because TE polarization in MDG has a high diffraction efficiency and it has been reported greatly in theoretical and experimental work, only TE polarization case is discussed in the following text.

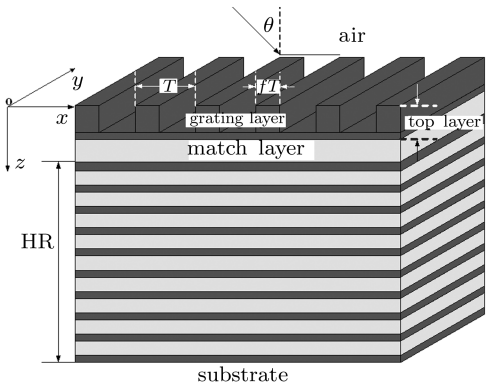


Fig. 1. Structure of the multilayer dielectric grating. The HR stack is composed of high refractive index layer H and low refractive index layer L. f is the grating filling factor.

By solving the eigenvalue equation of the multilayer waveguide thin-film stack situated between the cover and substrate layers, we can obtain all of waveguide modes in the MDG system. The propagation constant can be presented as

$$\beta_n = k_0\sqrt{\varepsilon_n}\sin\theta_n, \tag{3}$$

where $k_0 = 2\pi/\lambda$, λ is the wavelength in free space, ε_n and θ_n are the relative permittivity and the refraction angle in the nth layer, respectively. For each of β_n, the corresponding wave-vector component perpendicular to the layer boundary in waveguide thin-film stack, cover layer and substrate can be denoted by κ_n, κ_{c} and κ_{s}, and defined as[19]

$$\begin{aligned}\kappa_n &= (k_0^2\varepsilon_n - \beta_n^2)^{1/2},\\ \kappa_{\mathrm{c}} &= (\beta_n^2 - k_0^2\varepsilon_{\mathrm{c}})^{1/2},\\ \kappa_{\mathrm{s}} &= (\beta_n^2 - k_0^2\varepsilon_{\mathrm{s}})^{1/2},\end{aligned} \tag{4}$$

where ε_{c} and ε_{s} are the relative permittivities of cover layer and substrate, respectively.

The transmission matrix in the nth layer is expressed as[21]

$$\boldsymbol{M}_n = \begin{bmatrix} \cos(\kappa_n h_n) & -\dfrac{1}{\kappa_n}\sin(\kappa_n h_n) \\ \kappa_n \sin(\kappa_n h_n) & \cos(\kappa_n h_n) \end{bmatrix}, \quad (5)$$

where h_n is the physical thickness of the nth layer. As indicated in Ref. [21], the electric fields of cover and substrate are associated with the total transmission matrix $\boldsymbol{M}$ as follows:

$$\begin{bmatrix} E(h) \\ E(h)' \end{bmatrix} = \boldsymbol{M} \cdot \begin{bmatrix} E(0) \\ E(0)' \end{bmatrix} = \prod_{n=1}^{l} M_n \cdot \begin{bmatrix} E(0) \\ E(0)' \end{bmatrix}, \quad (6)$$

where h is the total thickness of waveguide. $E(0)$ and $E(h)$ are the transverse electric fields at the boundaries of cover layer and substrate, respectively, and $E(0)'$ and $E(h)'$ are the first derivative. The transverse electric fields in the cover layer and the substrate layer are given as

$$E(z) = \begin{cases} E(0)\exp(\kappa_{\rm c} z), & -\infty < z < 0, \\ E(h)\exp[-\kappa_{\rm s}(z-h)], & h < z < +\infty. \end{cases} \quad (7)$$

Inserting the transverse electric field, given in expression (7), into expression (6) yields

$$E(0)\begin{bmatrix} 1 \\ \kappa_{\rm c} \end{bmatrix} = \prod_{n=1}^{l} M_n \cdot \begin{bmatrix} 1 \\ -\kappa_{\rm s} \end{bmatrix} E(h). \quad (8)$$

If the incident intensity of cover is to vanish, which means $E(0) = 0$, then the electric field amplitude in the substrate must be zero. So the eigenvalue equation of the multilayer waveguide, in matrix form, is

$$\begin{bmatrix} -\kappa_{\rm c} & 1 \end{bmatrix} \prod_{n=1}^{l} M_n \begin{bmatrix} 1 \\ -\kappa_{\rm s} \end{bmatrix} = 0. \quad (9)$$

Expression (9) is the dispersion relation for waveguide mode that can be supported by the MDG structure. And it is related to the all parameters of MDG, including period, depth and duty cycle of corrugation, relative permittivities and thickness of high reflection multilayer, and so on. From detailed analyses of Eq. (9), it can be found that how each parameter of MDG influences the characteristic of the GMR in the MDG system. For the convenience of later discussion, the left side of Eq.(9) is defined as the function F as follows:

$$F = \begin{bmatrix} -\kappa_{\rm c} & 1 \end{bmatrix} \prod_{n=1}^{l} M_n \begin{bmatrix} 1 \\ -\kappa_{\rm s} \end{bmatrix}. \quad (10)$$

We also define the mode refractive index $N = \beta_n/k_0 = \sqrt{\varepsilon_n}\sin\theta_{\rm t}$ where $\theta_{\rm t}$ is named the guided-mode angle. In the MDG waveguide model, N always meets the following condition:[13]

$$\{\sqrt{\varepsilon_{\rm l}}, \sqrt{\varepsilon_{\rm eff}}\} < N < \sqrt{\varepsilon_{\rm h}}, \quad (11)$$

in which $\varepsilon_{\rm l}$ and $\varepsilon_{\rm h}$ are the relative permittivity of low refractive index material layer L and that of the high refractive index material layer H, respectively. The electrical fields in the L layer and the grating layer each are presented as an attenuation mode. So the factor κ_n in the elements of the transmission matrixes of the L layer and the grating layer can be set as

$$\kappa_n = {\rm i}\left(\beta^2 - k_0^2\varepsilon_n\right)^{1/2} = {\rm i}\alpha_n \quad (12)$$

and

$$\begin{aligned} \sin(\kappa_n h_n) &= {\rm i}\sinh(\alpha_n h_n), \\ \cos(\kappa_n h_n) &= \cosh(\alpha_n h_n), \end{aligned} \quad (13)$$

where ${\rm i} = \sqrt{-1}$ and $\alpha_n = \left(\beta^2 - k_0^2\varepsilon_n\right)^{1/2}$, so the transmission matrixes of the L layer and the grating layer become

$$M_i = \begin{bmatrix} \cosh(\alpha_i h_i) & -\dfrac{1}{\alpha_i}\sinh(\alpha_{\rm i} h_i) \\ -\alpha_i \sinh(\alpha_i h_i) & \cosh(\alpha_i h_i) \end{bmatrix}. \quad (14)$$

3. Inhibition of GMR

In the MDG structure, the high-order diffracted evanescent wave can excite the GMR. And the excited GMR condition is in the following form:[13]

$$N = \beta_n/k_0 = m\lambda/\Lambda - \sqrt{\varepsilon_{\rm c}}\sin\theta_{\rm i}, \quad (15)$$

where m is the diffracted order ($m = 0,\ \pm 1,\ \pm 2\ldots$), $\varepsilon_{\rm c}$ is the relative permittivity of the cover layer, Λ is the grating period, and $\theta_{\rm i}$ is the incidence angle. Here the incidence angle is defined as a negative value, and the diffraction angles are negative when they are located on the same side as incidence angle, otherwise as being positive. The necessary conditions which can excite the GMR are expressed as

$$\begin{aligned} &\max(\sqrt{\varepsilon_{\rm c}}, \sqrt{\varepsilon_{\rm s}}) \\ &< N < \max(\sqrt{\varepsilon_{\rm eff}}, \sqrt{\varepsilon_n} | n = 1, 2, 3\ldots). \end{aligned} \quad (16)$$

In the MDG structure, the highest relative permittivity is $\varepsilon_{\rm h}$, and the relative permittivity of substrate is larger than that of the cover layer that is

always air. For the MDG used in the CPA system, the period of grating is less than the wavelength used, and it has only 0th and –1st reflected diffraction orders. So the lowest high-order evanescent waves are +1st and –2nd. Then the necessary conditions for GMR become

$$\sqrt{\varepsilon_{\rm s}} < \lambda/\Lambda - \sqrt{\varepsilon_{\rm c}}\sin\theta_{\rm i} < \sqrt{\varepsilon_{\rm h}} \tag{17}$$

or

$$\sqrt{\varepsilon_{\rm s}} < |-2\lambda/\Lambda - \sqrt{\varepsilon_{\rm c}}\sin\theta_{\rm i}| < \sqrt{\varepsilon_{\rm h}}, \tag{18}$$

which means that at least one of the +1st and the –2nd order diffracted evanescent waves needs to meet the GMR conditions.

From inequalities (17) and (18) and according to Ref. [22], it is shown that reducing period of grating is an effective method to avoid the GMR's appearing in the required bandwidth both in angle and in wavelength.

And then for the 2nd component in inequalities (7) or (18), $\theta_{\rm i}$ changes within a reasonable range, $\theta_{\rm centre} \pm \Delta\theta$, in which broad-angular spectrum MDG requirement is satisfied. Here $\theta_{\rm centre}$ is the central incidence angle, θ_1 and θ_2 are defined as

$$\begin{aligned} |\theta_1| &= |\arcsin(n_{\rm h}\cdot\sin\theta_{\rm t} - \lambda/\Lambda)| \le |\theta_{\rm littrow}| - \Delta\theta, \\ |\theta_2| &= |\arcsin(n_{\rm h}\cdot\sin\theta_{\rm t} + 2\lambda/\Lambda)| \ge |\theta_{\rm littrow}| + \Delta\theta, \end{aligned} \tag{19}$$

in which the mode angle $\theta_{\rm t}$ is the maximum mode angle supported by the MDG structure and it can be calculated from the waveguide theory. θ_1 and θ_2 denote the incident angles at which GMR could be excited by +1st and –2nd order diffracted evanescent waves, respectively. When conditions (expression 19) are satisfied, all the incidence angles at which the GMR can be excited, are out of the range $\theta_{\rm centre} \pm \Delta\theta$. Based on expression (19), the maximum period of MDG can be obtained, which ensures that the MDG avoids the GMR at the incidence angle in the given range.

For an MDG design used in ultrashort pulse, high diffraction efficiency in the wavelength range $\lambda_0 \pm \Delta\lambda$ with no GMR is necessary, where λ_0 is central wavelength. First, it is needed to compare the values of $|3\sin\theta_{\rm i}|$ and $n_{\rm h}$, where $\theta_{\rm i}$ and $n_{\rm h}$ denote incidence angle and the highest index of all layers in MDG, respectively. When $|3\sin\theta_{\rm i}| > n_{\rm h}$, the maximum period of grating that ensures no GMR over the required wavelength range is given as follows:

$$\Lambda_{\max} = \frac{-2(\lambda_0 - \Delta\lambda)}{\sin\theta_{\rm i} - n_{\rm h}\cdot\sin\theta_{\rm t}}. \tag{20}$$

When $|3\sin\theta_i| < n_{\rm h}$, the expression for calculating the maximum period of grating is obtained to be

$$\Lambda_{\max} = \frac{\lambda_0 - \Delta\lambda}{\sin\theta_i + n_{\rm h}\cdot\sin\theta_{\rm t}}, \tag{21}$$

where $\theta_{\rm t}$ in Eqs. (20) and (21) are the maximum mode angle that can be supported by the MDG structure. And they can be calculated from waveguide theory.

As an example of expression (20), the central wavelength is 1040 nm, and the high diffraction efficiency bandwidth is 100 nm. The incidence angle $\theta_{\rm i} = 42°$, and the maximum mode angle $\theta_{\rm t} = 90°$. The highest refractive index $n_{\rm h}$ is 1.96 (HfO2), so the maximum period of grating is 753.1 nm. Under this period condition, there is no GMR in MDG over the wavelength range 1040±50 nm.

4. Numerical illustration

In this part, the numerical illustrations of GMR of MDG structure in angle spectrum and wavelength spectrum will be calculated from waveguide theory and FMM. And the results are compared and analysed. The physical process of each diffraction order excited GMR is clear.

4.1. Model

The MDG structure is shown in Fig. 1. The formula of HR stack is H(L2H) 9, where H denotes HfO_2 layer and $n_{\rm h} = 1.96$, L denotes SiO_2 , $n_{\rm l} = 1.46$, and optical thicknesses of H and L layer are both equal to a quarter of a reference wavelength (740 nm). Thicknesses of top layer and grating layer are the same, i.e. 240 nm (H material), and thickness of match layer is 30 nm (L material). The central wavelength of incident wave is 1040 nm, the period of grating is 847 nm and the corresponding Littrow angle is 37.9°. The fill factor of grating is $f = 0.35$. Refractive indexes of cover and substrate layers are $n_{\rm c} = 1$ and $n_{\rm s} = 1.52$, respectively.

4.2. GMR in angular spectrum

According to formula (15), the guided-wave mode angle $\theta_{\rm t}$ which can be excited by +1st and –2nd orders, is related to the incidence angle θ_i as shown in Fig. 2. When the incidence angle is in a range from $-75°$ to $-15°$, the guided-wave mode angle $\theta_{\rm t}$ would change in a range of 49°-to-90°). Then all guided-wave modes supported by the MDG structure can be

obtained from function F (see expression (10)) with $\theta_{\rm t}$ in the range of 49°-to-90°, shown in Fig. 3.

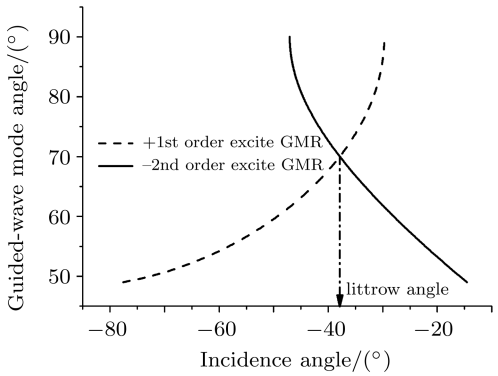


Fig. 2. Guided-wave mode angle versus incidence angle at which GMR in +1st order or –2nd order can be excited.

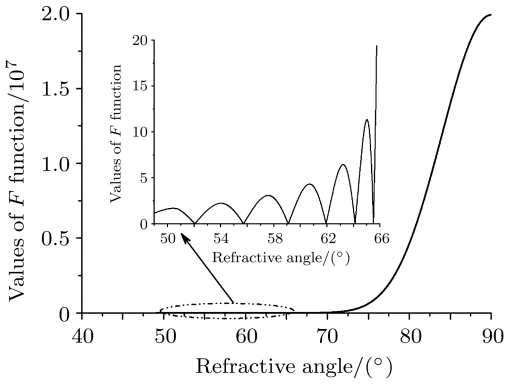


Fig. 3. Value of F function versus refractive angle θ_n, with incidence wavelength being 1040 nm.

Figure 3 presents the curve of F function value versus refraction angle θ_n. When F value is 0, the refraction angle is the guided-wave mode angle $\theta_{\rm t}$ in MDG waveguide. It is shown that F value increases rapidly when θ_n is larger than the maximum of $\theta_{\rm t}$. Thus, the guided-wave mode is present only when the mode angle $\theta_{\rm t}$ is less than 66° within the given model parameters. The inset in Fig. 3 shows all guide-wave modes. The maximum $\theta_{\rm t}$ in expression (19) can be obtained from Fig. 3 too.

Combining the results in Fig. 3 with GMR conditions as shown in expression (15), the incidence angle at which the GMR is excited, can be calculated. The effect of the incidence angle on the value of function F is shown in Fig. 4, where the solid line and dash line represent the values of function F excited by +1st order and –2nd order, respectively. This result can also be seen from Figs. 2 and 3. When the mode angle $\theta_{\rm t}$ is less than 66°, one guided-wave mode angle corresponds to two excite orders (+1st order and –2nd order). The incidence angles exciting GMR in +1st order are less than the Littrow angle and those exciting GMR in –2nd order are larger than the Littrow angle.

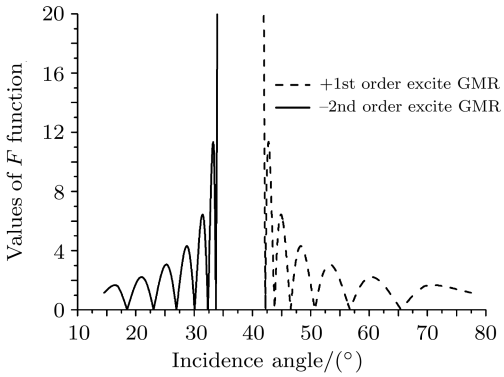


Fig. 4. Effect of incidence angle on the value of function F, calculated by waveguide theory.

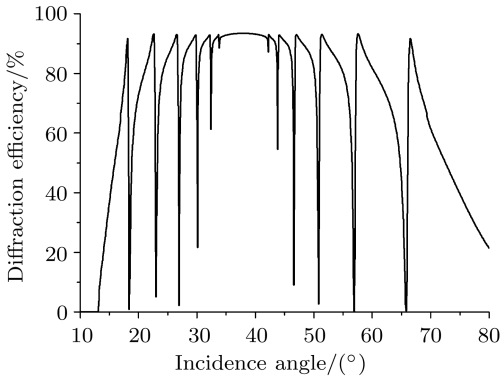


Fig. 5. Diffraction efficiency versus incidence angle spectrum, calculated by FMM.

Figure 5 shows the relationship between diffraction efficiency of MDG and incidence angle, which is calculated by FMM. GMR phenomena are demonstrated obviously. By comparing Fig. 4 with Fig. 5, it can be found that the incidence angles exciting GMR calculated by waveguide theory and by FMM are coincident. However, the waveguide theory provides a clearer physical process and gives the exciting order of each GMR exactly. These are helpful for us to understand the GMR phenomenon and analyse how each parameter of MDG affects the characteristic of GMR.

The electric field in MDG is calculated by FMM as shown in Fig. 6. Figures 6(a) and 6(b), which are corresponding to GMRs excited by +1st and –2nd order diffraction evanescent waves, respectively. The incidence angles are the same with respect to the GMR position in Fig. 5. It can be found that when the guided-mode angle descends (from right to left), the guided modes in MDG are marked by 0, 1,

2 . . . sequentially. For a high order mode, the incident light forms a standing wave in MDG, and the 0-value points of standing wave are distributed averagely on the z axis of MDG. So the characteristic of guided mode in MDG is similar to that in a single layer slab waveguide.

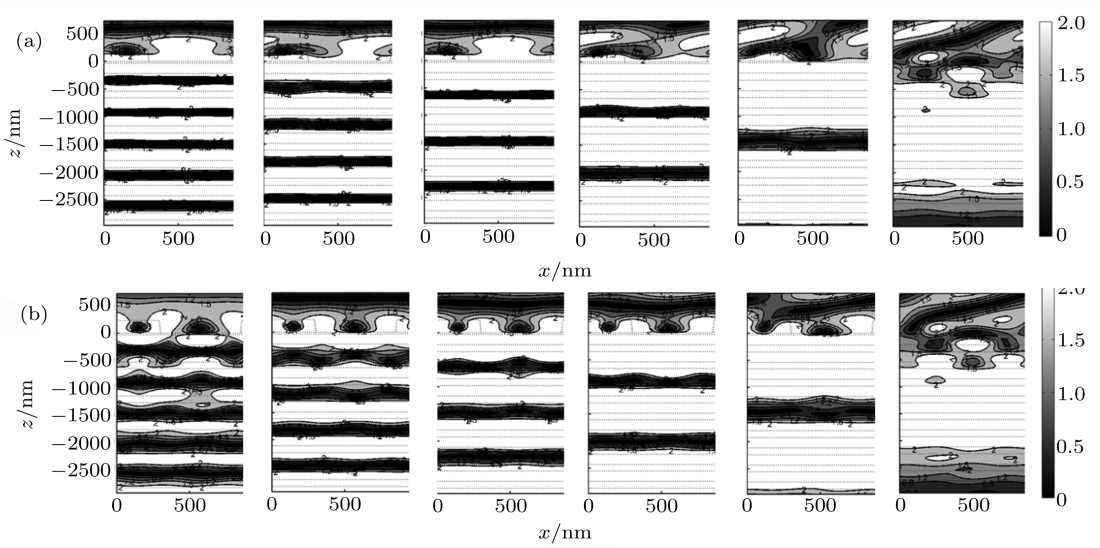


Fig. 6. Electric fields in MDG, where GMRs are excited in +1st order, with incidence angles being 18.4°, 23°, 26.9°, 30.1°, 32.4°, and 33.8°, from left to right sequentially (a), and in –2nd order, with incidence angles being 65.8°, 56.9°, 50.8°, 46.6°, 43.8°, and 42.2°, sequentially. The wavelength of incidence light is 1040 nm.

There are some guide-wave channels in MDG, where the electric fields are enhanced. So it is demonstrated that the existence of GMR in MDG not only destroys the pulse shape (as shown in Fig. 5), but also reduces the LIDT of MDG.

By comparing the electric fields in MDG, which are shown in Figs. 6(a) and 6(b), it is also found that when the light is incident upon MDG at two different incidence angles at which the GMR in +1st and –2nd orders is excited and the corresponding guided-mode angles are the same, then the characteristics of electric fields in MDG are equivalent.

4.3. GMR in wavelength spectrum

For a given wavelength range, the corresponding range of guided-wave mode angle $\theta_{\rm t}$ at which the GMR in +1st order and –2nd order can be excited, can be calculated by GMR conditions. For the incident light exciting the GMR in a wavelength range of 1040±90 nm, the values of mode angle $\theta_{\rm t}$ are in ranges of (62°, 90°) and (56°, 90°) corresponding to +1st and –2nd order exciting (as shown in Fig. 7), respectively.

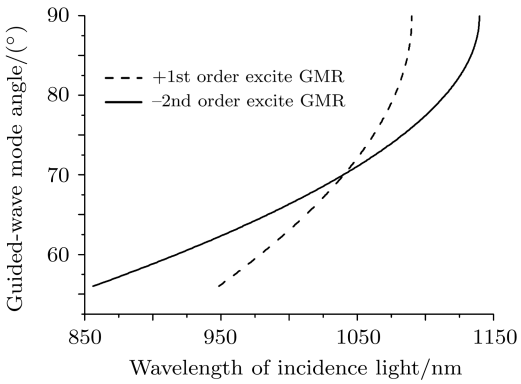


Fig. 7. Spectra of the incidence wavelength versus guided-wave mode angle excited in +1st and –2nd orders.

Figure 8(a) shows the relationship between the value of F function and refractive angle θ_n. For each wavelength, the corresponding diffracted angles of diffracted orders are different from each other, and thus the mode angles are not the same. The values of function F excited by +1st and –2nd order are shown with the solid line and the dash line in Fig. 8(a), respectively. There is no more 0 value for function F when the mode angle is larger than 66°. Taking each guided-wave mode $\theta_{\rm t}$ into consideration of the GMR

condition given expression (15), the incidence wavelength excited GMR in +1st –and 2nd orders can be obtained as shown in Fig. 8(b). The wavelengths at which the GMR in two orders can be excited, are less than the central wavelength 1040 nm, and this is consistent with the result shown in Fig. 7.

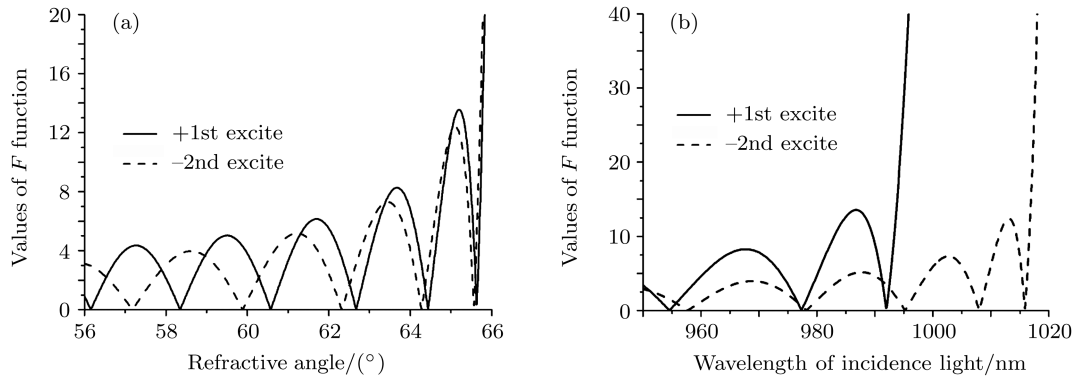


Fig. 8. Values of function F versus refractive angle in two orders (a) and incidence wavelength in two orders (b), which are calculated from waveguide theory.

Diffraction efficiency calculated by FMM is shown in Fig. 9. By comparing Figs. 8(b) and 9(a), it can be found that the incidence wavelengths at which the GMR can be excited, calculated from waveguide theory are in good agreement with those by FMM. Just as indicated by the above analysis, there exists no more GMR when the incidence wavelength is longer than the central wavelength 1040 nm, which is shown in Fig. 9(b).

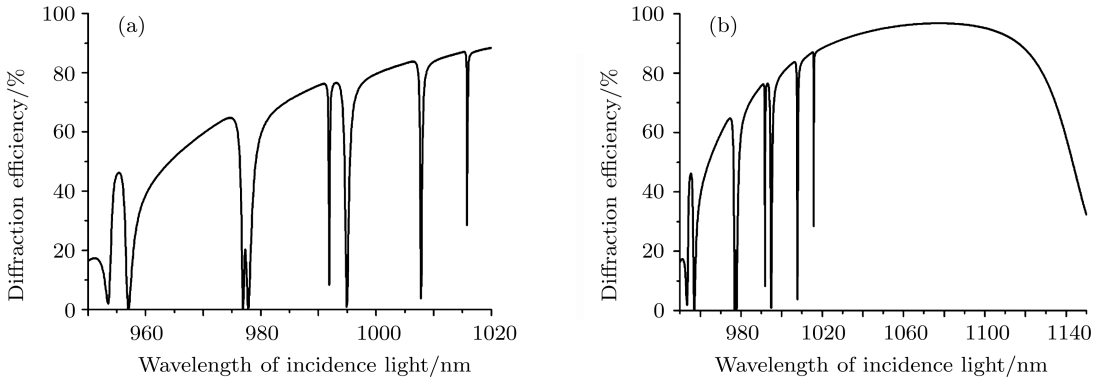
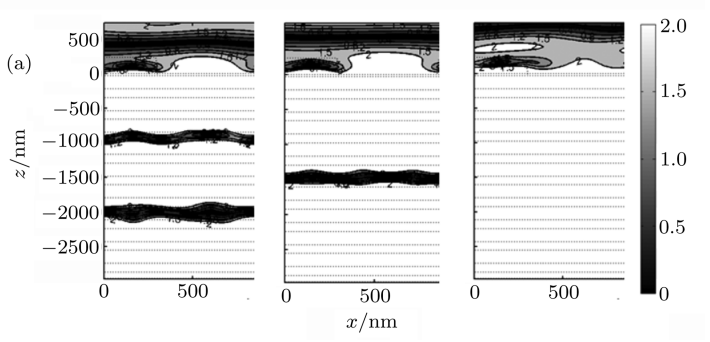


Fig. 9. Spectra of diffraction efficiency in wavelength ranges of 950 nm–1020 nm (a) and 950 nm–1150 nm (b), which are obtained by FMM.

Figure 10 illustrates the electric fields in MDG according to diffracted incident light at an incidence angle of 37.9°. Figures 10(a) and 10(b) correspond to GMR excited by +1st and –2nd order diffraction evanescent waves, respectively. The wavelength of incident light may be found in Fig. 9. For the GMRs with the same guided-mode angles, the electric fields in MDG are similar (Fig. 10(a) and the right three panels in Fig. 10(b)). It is shown obviously that the electric field is enhanced in MDG.



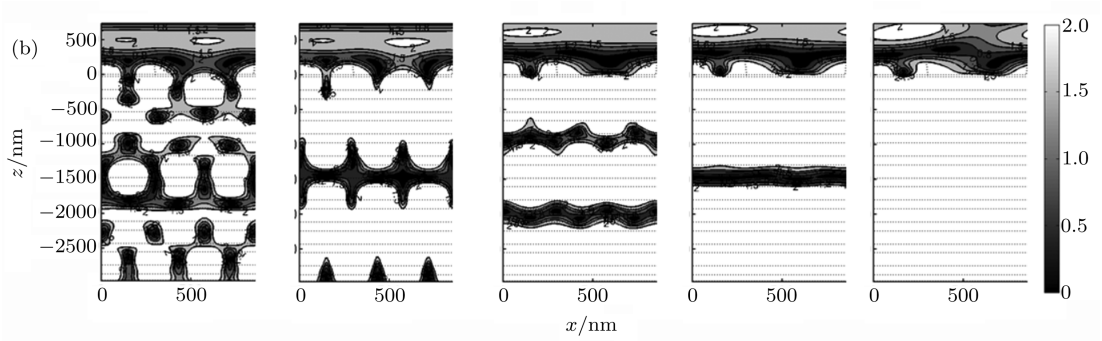


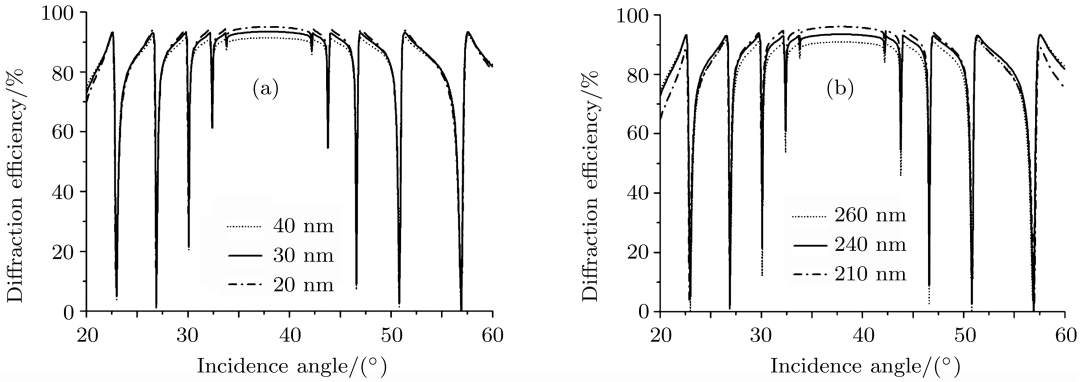
Fig. 10. Electric fields in MDG, where GMR is excited by +1st order, with wavelengths of incidence light being 953.5 nm, 976.9 nm, 991.9 nm, respectively (from left to right) (a) by -2nd order, with wavelengths of incidence light being 957 nm, 977.8 nm, 994.9 nm, 1007.8 nm, and 1015.8 nm, respectively. The incidence angle at 37.9°.

5. Effects of MDG parameters on characteristic of GMR

By comparing the GMR analysis obtained from the waveguide theory and that calculated by FMM in the above, it is found that waveguide theory provides a clear physical process of GMR and the exciting diffracted orders corresponding to each guided wave mode are also obtained exactly. These advantages of waveguide theory are very helpful for us to analyse how the parameters affect the characteristic of GMR. Based on the waveguide theory, the relationships between the characteristic of GMR and some parameters of MDG, including period of grating, fill factor, thickness of grating layer and so on, will be discussed in detail here. The basic parameters for numerical calculation are the same as those given in Section 4.1. In order to compare the changes of characteristic of GMR clearly, GMR in angular spectrum calculated by FMM will be shown in this section.

The parameters of grating and match layers are the main factors for obtaining a high-diffraction-efficiency broad-bandwidth MDG.[6−9,23] So how to choose these parameters, such as the period of grating, fill factor, thicknesses of grating layer and match layer, impact GMR of MDG system should be discussed. And it would be great helpful for us to design excellent broad bandwidth MDG without GMR appearing.

Combining the EMT expression (1) with the given parameters of MDG, it can be deduced that the refractive indexes of grating layer and low refractive index layer (including match layer) are lower than the guided-wave mode refractive index N at which the GMR in +1st order and −2nd order is excited. The electric fields in grating layer and match layer are both in attenuation modes. And the grating layer and match layer are located in the outermost two layers of MDG system, so the guide-wave modes in these two layers present the leaky modes, and the thicknesses of these two layers do not exert an influence on the GMR very much, which is shown in Figs. 11(a) and 11(b) clearly.



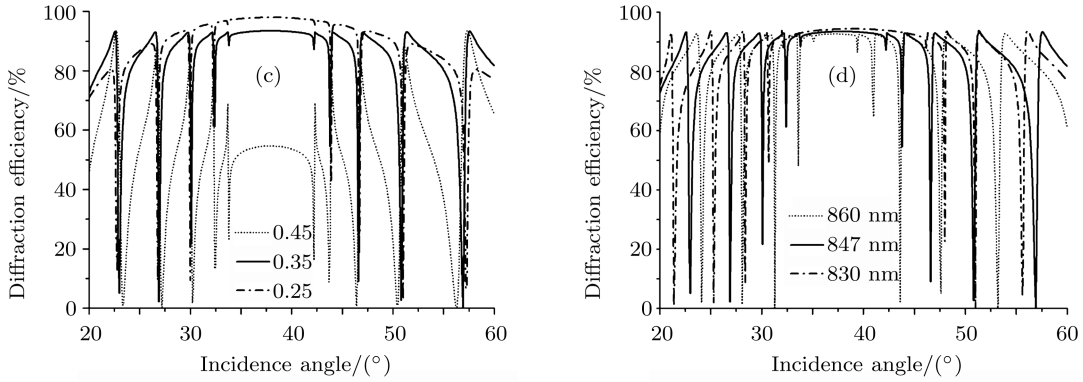


Fig. 11. Effects of grating layer and match layer on the characteristic of GMR of MDG system, showing the incidence angles at which GMR is excited when different values are set to grating layer thickness, match layer thickness, fill factor and period of grating, correspondingly.

The fill factor of MDG is a very important parameter. It determines the diffraction efficiency of MDG and the electric field intensity on the grating ridge which affects the LIDT of MDG.[7,23] So the fill factor is always considered carefully when the MDG is designed. The refractive index of ridge part of grating is 1.96 (HfO_2). Based on the given basic parameters, when the fill factor changes from 0.25 to 0.5, the effective refractive index of grating layer obtained from expression (1) is in a range of 1.13–1.25), which is lower than the guided-wave least mode index N (1.61) of MDG system. So the electric field of grating layer is always in an attenuation mode. And thus the fill factor changes in a range of 0.25–0.5), and the incidence condition corresponding to the GMR does not change obviously as shown in Fig. 11(c). But if the refractive index of grating layer is higher and/or the fill factor is larger, the grating layer turns into a guided-wave layer. Under this situation, the fill factor and the thickness of grating would become more influential on the GMR of MDG system.

The GMR condition will be not satisfied when the period of grating reduces, and there will appear no GMR in the required bandwidth (as discussed in Section 3). From the EMT expression (1), the variation of grating period does not change the effective refractive index of grating layer, and thus it does not influence the guided-wave mode in MDG system. But based on the GMR conditions, if there is a guided-wave mode excited in MDG system, the corresponding incidence exciting condition (both in angle and in wavelength) will change as the period of grating is different. And when the period of grating decreases and the other parameters are kept unchanged, the incidence angles at which the GMR in +1st on –2nd orders can be excited, deviate from the Littrow angle as shown in Fig. 11(d), and the incidence wavelengths also deviates from the central wavelength.

Another group of important factors of MDG are the properties of high (H) and low (L) refractive index layers which comprise the HR thin film stack, including physical thicknesses and refractive indices of these two kinds of layers. As shown in Fig. 12(a), the incidence angle exciting GMR becomes close to the Littrow angle as the thickness of H layer increases. Contrarily, the incidence angle deviates from the Littrow angle as the thickness of H layer reduces. There are some different situations for L layer. As shown in Fig. 12(a), when the thickness of H layer increases, the incidence angle exciting GMR is close to the Littrow angle as incidence angle is near by the Littrow angle, however, the incidence angle exciting GMR deviates from the Littrow angle as incidence angle is away from Littrow angle. It is shown more clearly in Fig. 13 in which the GMR position is presented in the eigenvalue form. The physical origin of such a phenomenon is under study. But it is revealed that the combination of thinner H layer and thicker L layer is conducive to keeping the incidence angle exciting GMR away from Littrow angle. This is useful for the broad band angular spectral design. The same conclusion can be extended to broad band spectral MDG design.

Figures 12(c) and 12(d) show the angular spectrum according to the refractive indices of H and L layers, respectively. It is found that the difference in refractive index leads to a great change in GMR characteristic of the MDG system. When the refractive index varies greatly, the result of eigenequation of MDG system turns quite different. Especially, as the refractive index of H layer increases, the GMR con-

ditions is matched in wider incidence conditions.[22] And thus there are more GMR positions in a diffraction efficiency spectrum as shown in Fig. 12(c). So when the different materials are chosen for MDG design, the characteristic of GMR should be discussed carefully.

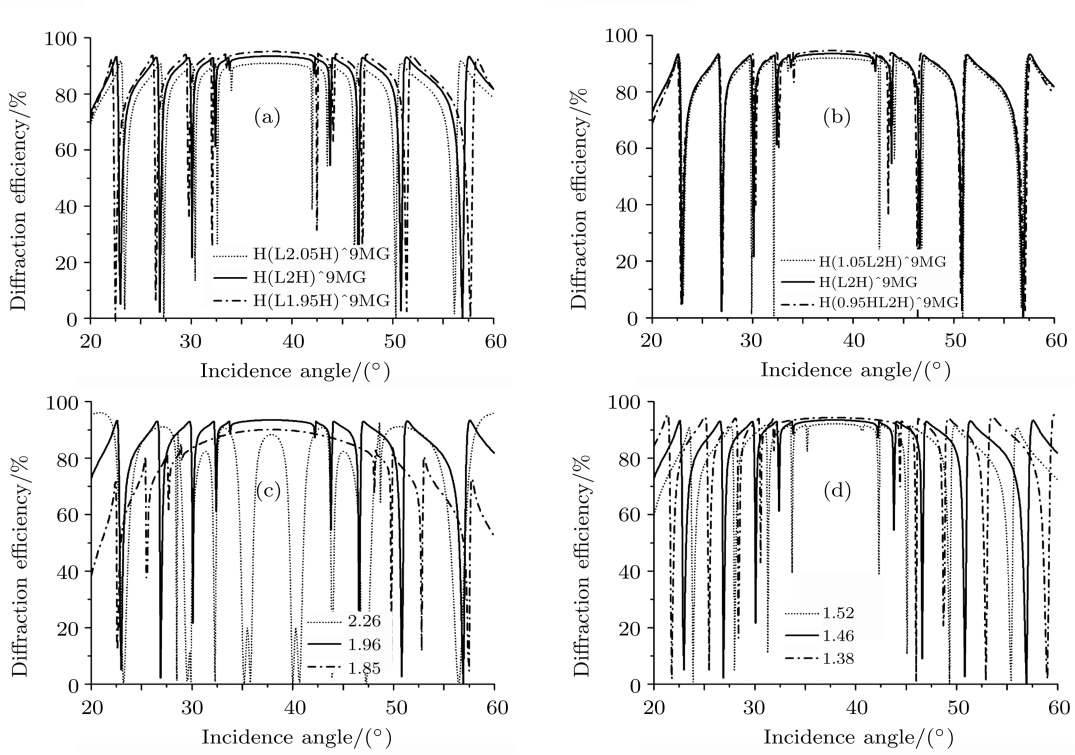


Fig. 12. Effects of parameters of high (H) and low (L) refractive index layers on the characteristic of GMR of MDG system, showing the incidence angle at which GMR is excited when different values are set to the H layer thickness, L layer thickness, and H layer refractive index ($n_{\rm H} = 1.85$, 1.96, 2.26) and L layer refractive index ($n_{\rm L} = 1.38$, 1.46, 1.52), respectively.

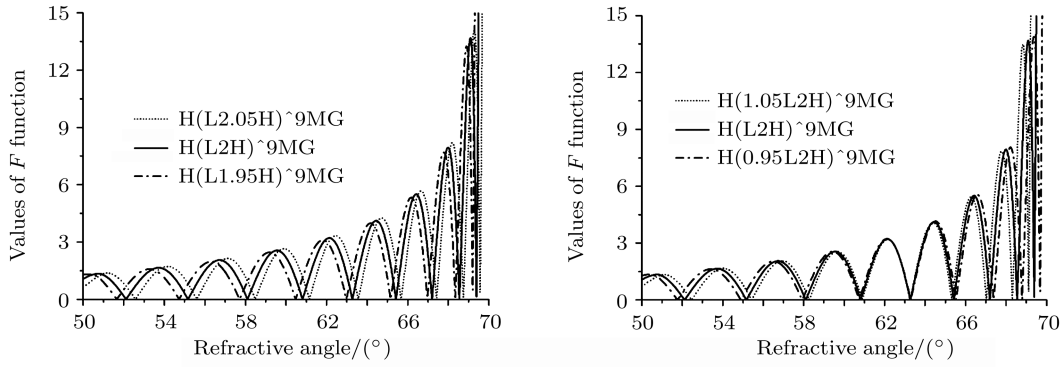


Fig. 13. Values of function F corresponding to the refractive angle θ_n with incidence wavelength being 1040 nm.

Furthermore, for a design of broad-band high-efficiency MDG, it is required that the HR mirror should provide a high reflectivity in the broad band range. There are three methods that are usually employed to widen the bandwidth of HR mirror. The first method is to increase the repeat time of the basic film (HL or H2L), and shape the reflection efficiency spectrum into a rectangle form, so it provides nearly 100% reflection efficiency in a broader range. The second method is to increase the difference in refractive index between H layer and L layer, so the high-efficiency bandwidth of HR stack is widened. And the third method is to overlap two HR stacks with different central wavelengths. The third method is a common method of widening the bandwidth of HR thin film.

But if the period of grating is not small enough to avoid the GMR, these three methods cannot be used to well achieve a broadband MDG. For the first method, the increasing of repeat time of basic film can lead to an increase in the number of layers in MDG, which can support the guided-wave mode, and thus there will exist more GMRs in the MDG system as shown in Fig. 14. And for the second method, because the low refractive index material is always SiO_2 with $n_L = 1.46$ (based on our fabrication condition), the increasing of the difference in refractive index between H layer and L layer means that a higher refractive index material is used in the H layer. As analysed before, the introduction of higher refractive index material into MDG might lead to more GMRs. The problem of the third method is the same as that of the first one, and more layers can induce more GMRs. So when the period is not small enough, these three ways can all bring about more GMRs. Therefore, before MDG design, it should consider the period of grating first, thereby ensuring that the bandwidth of HR mirror could be fully used.

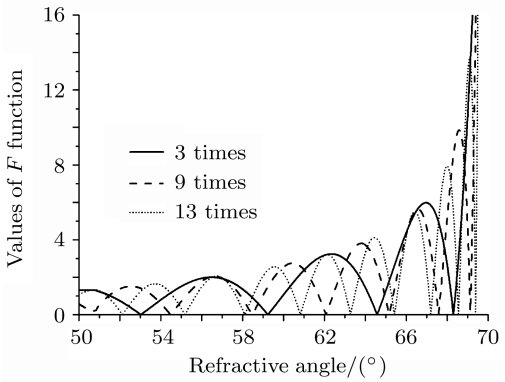


Fig. 14. The number of guided-wave modes corresponding to the repeat time of basic film stack (H2L).

6. Conclusion

In this paper, all GMRs supported by an MDG system are found based on the waveguide theory. The incidence positions corresponding to each GMR are also obtained. The results calculated from the waveguide theory are consistent with those obtained by FMM. And the waveguide theory provides a clear physical process of GMR, and it is useful to analyse the effect of each grating parameter on the characteristics of GMR.

The electric field in the MDG is shown to be enhanced obviously, and the characteristics of the guided mode in MDG is also found to be similar to that in a single layer slab waveguide.

From the discussion on each parameter of grating, it is found that the period plays an important role in the GMR characteristic of the MDG system. When period is increased, the incidence angle (wavelength) at which GMR can be excited, becomes close to the Littrow angle (centre wavelength) and the diffraction bandwidth turns narrow. The variations of fill factor, thickness of grating layer and match layer do not affect the GMR so much. The combination of thinner H layer and thicker L layer leads incidence angle (wavelength) to deviate from the Littrow angle (central wavelength). That is conducive to widening the diffraction bandwidth. Higher refractive index of H layer might bring about more GMRs in the MDG system.

Three methods to widen bandwidth of HR mirror can all induce more GMRs. Thus the period of grating should be considered carefully to ensure that the bandwidth of HR mirror can be used well.

The other important result is that reducing period can eliminate the excitation of GMR effectively. And the expressions of maximum period of MDG are deduced. These are very meaningful for the design of broad-bandwidth high-efficiency MDG.

References

[1] Pessot M, Squier J, Mourou G and Harter D J 1989 *Opt. Lett.* **14** 797

[2] Perry M D, Boyd R D, Britten J A, Shore B W, Shannon C and Li L 1995 *Opt. Lett.* **20** 940

[3] Shore B W, Perry M D, Britten J A , Boyd R D, Feit M D, Nguyen H T, Chow R, Loomis G and Li L 1997 *J. Opt. Soc. Am.* A **14** 1124

[4] Lu P P, Sun K X, Byer R L, Britten J A, Nguyen H T, Nissen J D, Larson C C, Aasen M D, Carlson T C and Hoaglan C R 2009 *Opt. Lett.* **34** 1708

[5] Stuart B C, Feit M D, Herman S, Rubenchik A M, Shore B W and Perry M D 1996 *Phys. Rev.* B **53** 1749

[6] Canova F, Clady R, Chambaret J P, Flury M, Tonchev S, Fechner R and Parriaux O 2007 *Opt. Express* **15** 15324

[7] Flury M, Tishchenko A V and Parriaux O 2007 *J. Lightwave Technol.* **25** 1870

[8] Flury M, Tonchev S, Fechner R, Schindler A and Parriaux O 2007 *J. Eur. Opt. Soc. Rap. Public.* **2** 7024
[9] Lyndin N, Flury M, Tonchev S, Fechner R and Parriaux O 2007 *J. Eur. Opt. Soc. Rap. Public.* **2** 7019
[10] Hessel A and Oliner A A 1965 *Appl. Opt.* **4** 1275
[11] Magnusson R and Wang S S 1992 *Appl. Phys. Lett.* **61** 1022
[12] Wang S S and Magnusson R 1993 *Appl. Opt.* **32** 2606
[13] Wang S S and Magnusson R 1995 *Appl. Opt.* **34** 2414
[14] Wang Z, Sang T, Wang L, Zhu J, Wu Y and Chen L 2006 *Appl. Phys. Lett.* **88** 251115
[15] Fu X, Yi K, Shao J and Fan Z 2009 *Opt. Lett.* **34** 12
[16] Ma J Y, Liu S J, Zhang D W, Yao J K, Xu C, Jin Y X, Shao J D and Fan Z X 2008 *Chin. Phys.* B **17** 3704
[17] Wei C, Liu S, Deng D, Shen J, Shao J and Fan Z 2006 *Opt. Lett.* **31** 1223
[18] Ma J Y, Liu S J, Wei C Y, Jin Y X, Zhao Y A, Shao J D and Fan Z X 2008 *Acta. Phys. Sin.* **57** 827 (in Chinese)
[19] Okamoto K 2005 *Fundamentals of Optical Waveguides* (2nd ed) (New York: Academic) p16
[20] Li L 1993 *J. Opt. Soc. Am.* A **10** 2581
[21] Born M and Wolf E *Principles of Optics* (7th ed) (Cambridge: Cambridge University Press) p901-904
[22] Wang J, Jin Y, Ma J, Shao J and Fan Z 2010 *Chin. Phys.* B (to be published)
[23] Wei H and Li L 2003 *Appl. Opt.* **42** 6255